Electronic Supplementary Information

Sustainable Poly(butylene furanoate)/Carbon Nanotube Composite Fibers for Wearable Thermoelectric Generator

Yi-Hsuan Huang,[a] Chih-Wei Hsu,[a] Cheng-Yuan Lin,[a] Jhih-Min Lin,[b] Guang-Way Jang,[c] Yung-Pin Huang,[c] Shih-Huang Tung,[d] and Cheng-Liang Liu, *[ade]

[a] Department of Materials Science and Engineering, National Taiwan University, Taipei 10617, Taiwan

[b] National Synchrotron Radiation Research Center, Hsinchu, 30076, Taiwan

[c] Material and Chemical Research Laboratories, Industrial Technology Research Institute, Hsinchu, 300044, Taiwan

[d] Institute of Polymer Science and Engineering, National Taiwan University, Taipei 10617, Taiwan

[e] Advanced Research Center for Green Materials Science and Technology, National Taiwan University, Taipei 10617, Taiwan

KEYWORDS. poly(butylene furanoate), carbon nanotubes, wet spinning, thermoelectric generator, wearable

Characterization. The microstructure of the composite fibers was characterized by a HITACHI S-4800 field emission scanning electron microscope (FE-SEM). Cross-section area (*A*) of the composite fibers was obtained JSM-6510 using scanning electron microscope. Differential scanning calorimetry (DSC) was obtained by Discovery DSC 25 from TA Instrument. Microbeam X-ray diffraction (XRD) experiments were conducted at the TPS 25A beamline of the National Synchrotron Radiation Research Center (NSRRC) in Hsinchu, Taiwan, using an X-ray wavelength of 0.826 Å. Raman spectroscopy from Renishaw with an excitation wavelength of 532 nm was employed. Mechanical properties of the composite fibers were evaluated by EZ-Test universal testing machine (SHIMADZU) at a speed of 1 mm min^{-1}.

Table S1. Reported values of the Seebeck coefficient and the corresponding *ΔV* from TEGs placed on the human wrist in previous studies.

Sample	Seebeck coefficient ($\mu V\ K^{-1}$)	*ΔV* while wearing on wrist (mV)	Reference
PANI/SWCNT (p-type)	30.8	0.23	[1]
PEDOT:PSS/DMSO (p-type)	19	0.11	[2]
PEDOT:PSS/WPU (p-type)	19	0.44	[3]
PEDOT:PSS/SWCNT (p-type)	27.1	0.22	[4]
PBF/SWCNT (p-type)	26.0 ± 1.2	1.5	This work
PBF/SWCNT (n-type)	–18.6 ± 1.8		

Table S2. Mechanical properties of composite fibers under different post annealing conditions.

Composite fibers	Tensile stress (MPa)	Young's modulus (MPa)	Elongation (%)
1:1 w/o	28.9	2417	6.09
1:1 100	41.9	2942	6.52
1:1 150	43.2	3410	4.87

Table S3. Thermoelectric properties of composite fibers under different post annealing conditions.

Composite fibers	Conductivity (S cm^{-1})	Seebeck coefficient (μV K^{-1})	Power factor (μW m^{-1} K^{-2})
1:1 w/o	42.9 ± 2.7	22.3 ± 0.2	2.13 ± 0.1
1:1 100	98.2 ± 27.7	23.5 ± 0.2	5.44 ± 1.51
1:1 150	113.0 ± 11.6	26.0 ± 1.2	7.60 ± 0.79
2:1 w/o	12.0 ± 1.37	22.1 ± 1.1	0.58 ± 0.01
3:1 w/o	8.35 ± 0.01	21.9 ± 1.1	0.401 ± 0.04

Table S4. Reported value of Power factor, Young's modulus and Elongation at break of carbon nanotube-based fibers in previous studies.

Materials	Power factor ($\mu W\ m^{-1}\ K^{-2}$)	Young's modulus (GPa)	Elongation at break (%)	Reference
SWCNT	26.25	16.39	3.25	[5]
CNT/WPU/PVA	1.78	0.44	27	[6]
CNT	2810	22.5	2	[7]
CNT yarn	2250	90	2	[8]
PBF/SWCNT	7.60 ± 0.79	3.41	4.87	This work

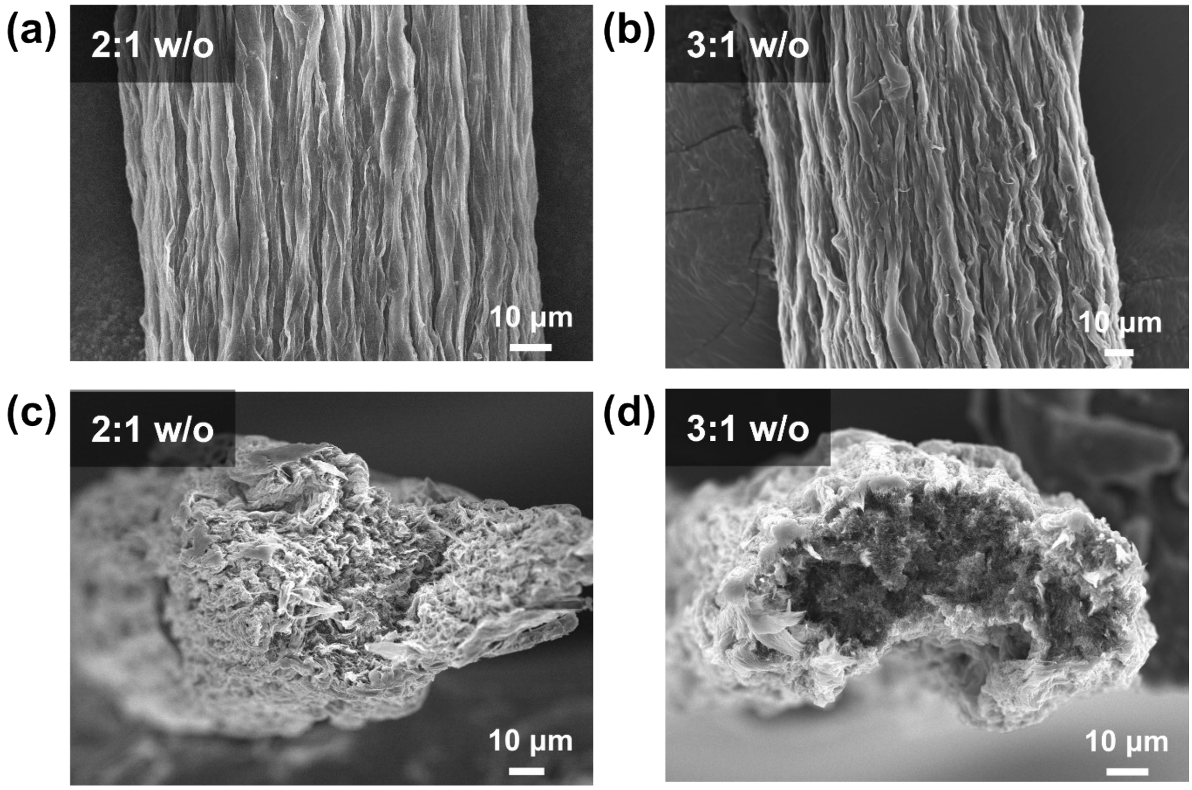

Fig. S1. SEM images of (a) 2:1 w/o and b 3:1 w/o composite fibers. Cross-sectional SEM images of c 2:1 w/o and d 3:1 w/o at 1000× magnification.

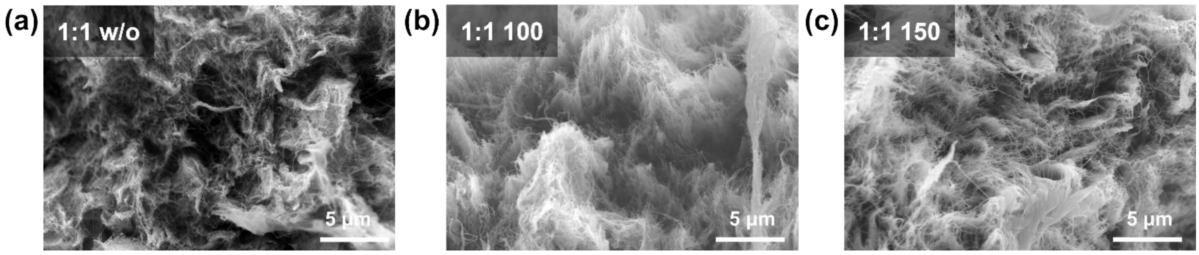

Fig. S2. Cross-sectional SEM images of (a) 1:1 w/o, (b) 1:1 100 and (c) 1:1 150 composite fibers at 5000× magnification.

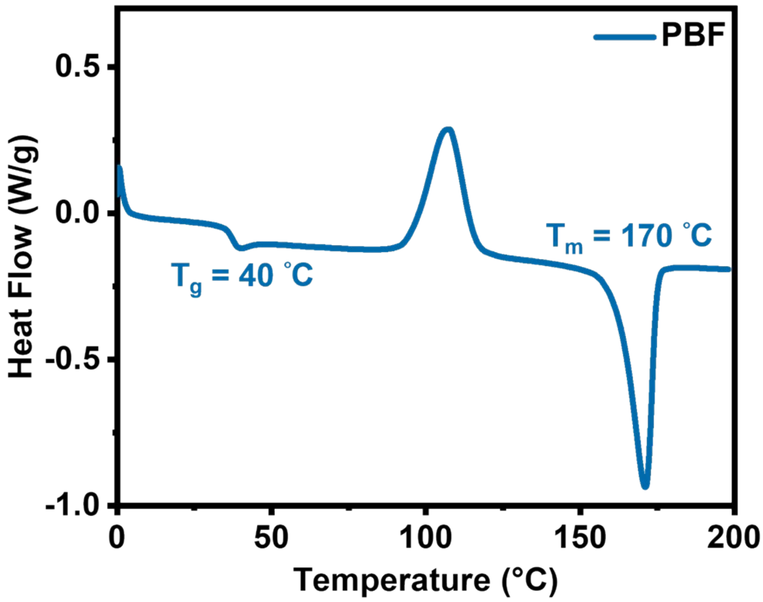

Fig. S3. The DSC thermogram of pristine PBF.

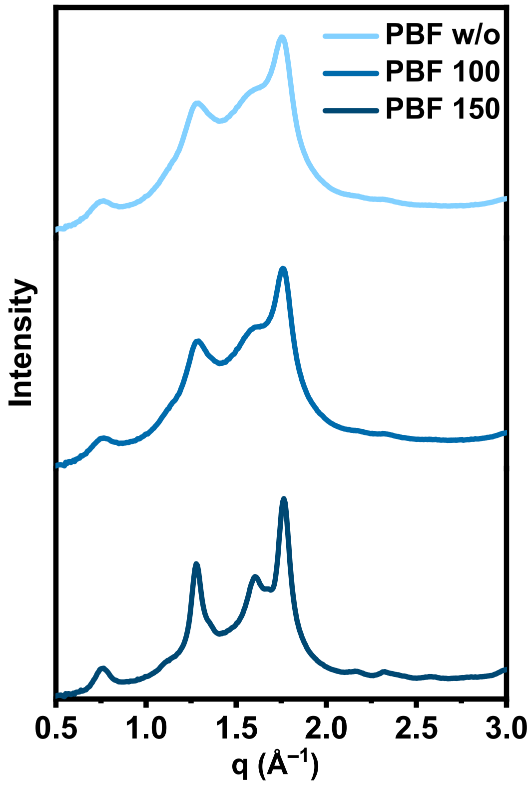

Fig. S4. Diffraction profiles of pristine PBF fibers with different annealing processes.

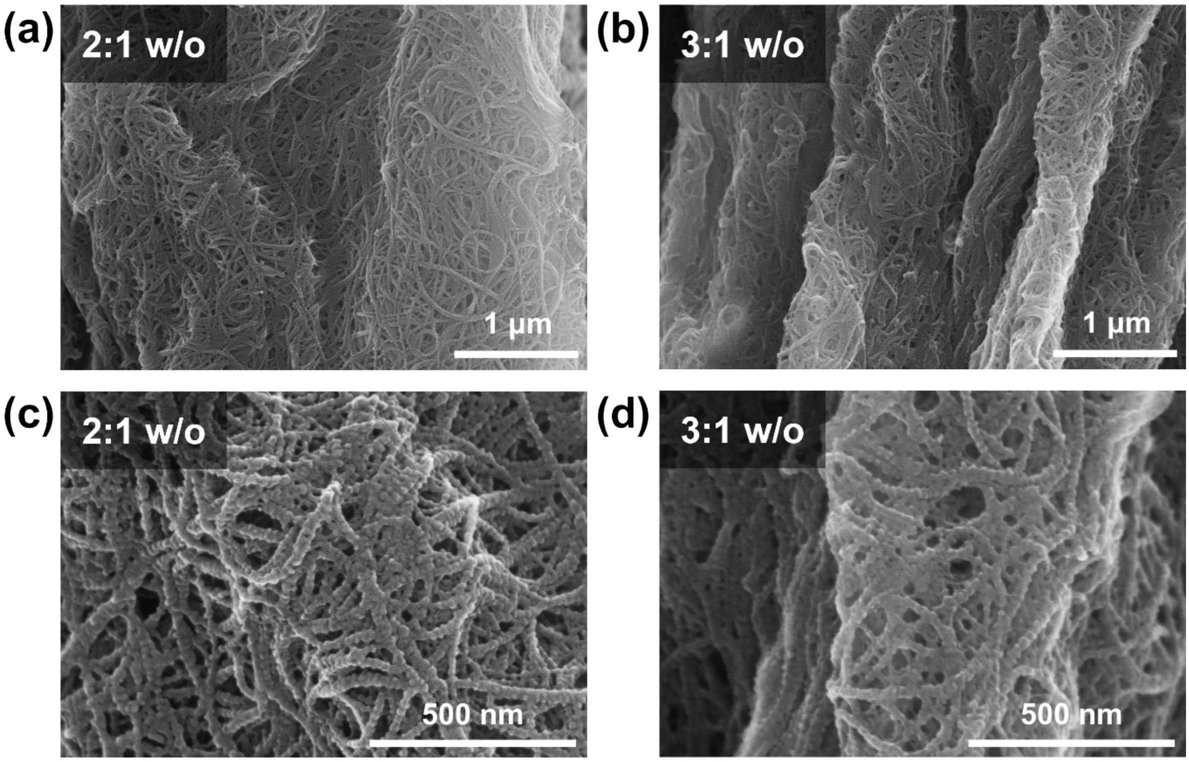

Fig. S5. SEM image of 2:1 w/o and 3:1 w/o composite fibers at (a, b) 30k× and (c, d) 100k× magnification.

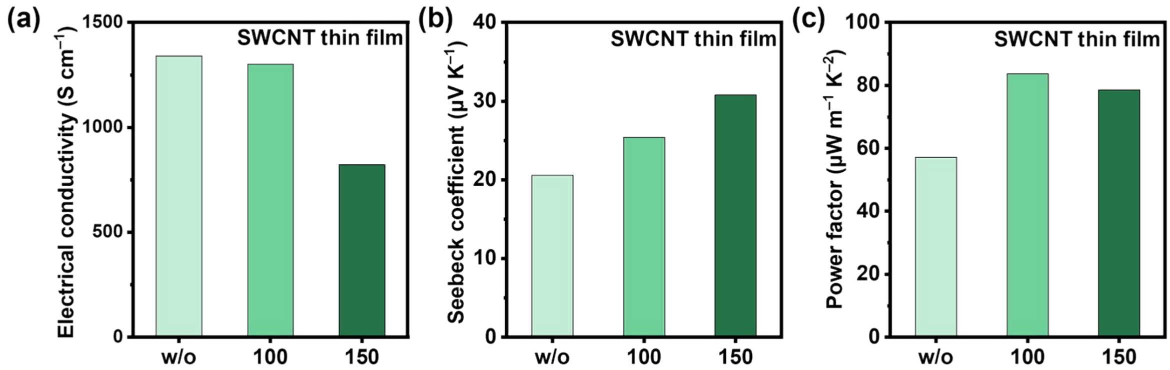

Fig. S6. Thermoelectric performance of SWCNT thin films with different annealing temperatures: (a) electrical conductivity, (b) Seebeck coefficient and (c) power factor.

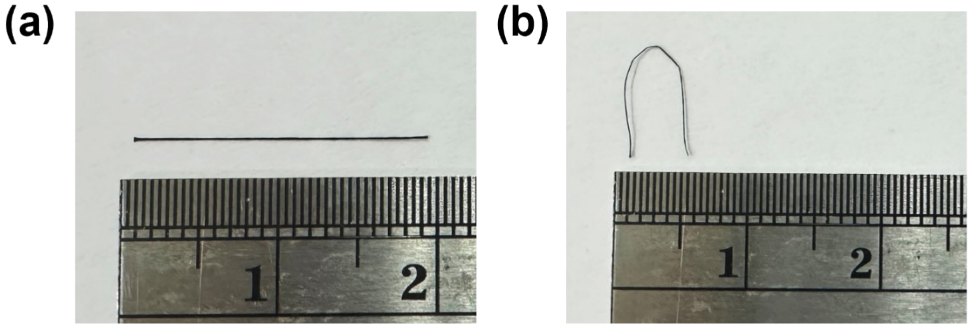

Fig. S7. Photograph images of the composite sample (a) before and (b) after bending.

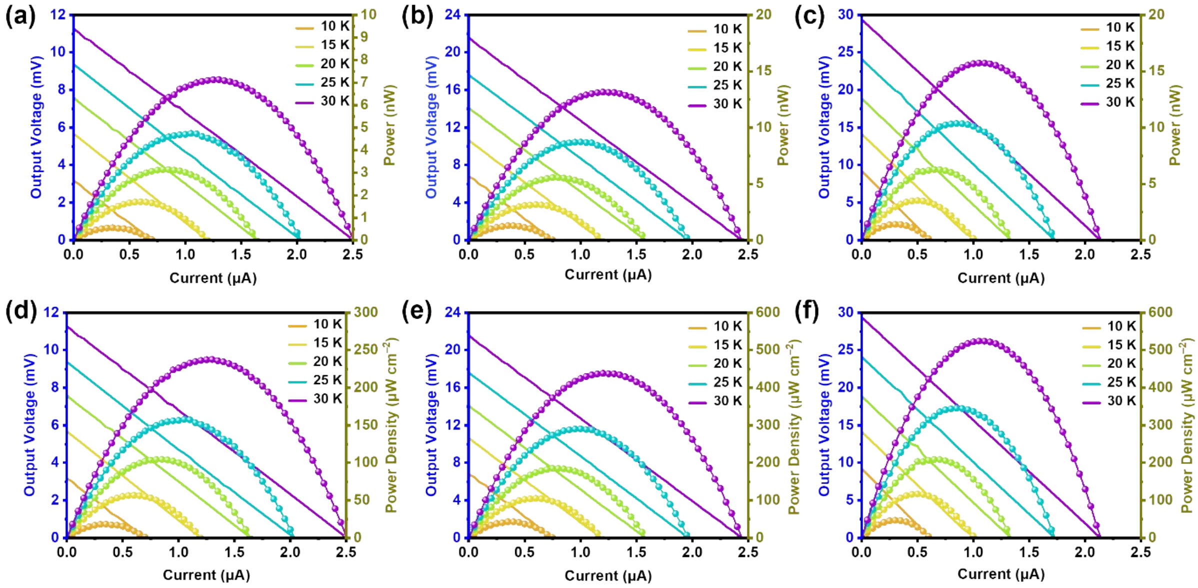

Fig. S8. The output voltage and power characteristics of TEG with 10 junctions (a, b), 20 junctions (c, d) and 30 junctions (e, f) under varying temperature gradients.

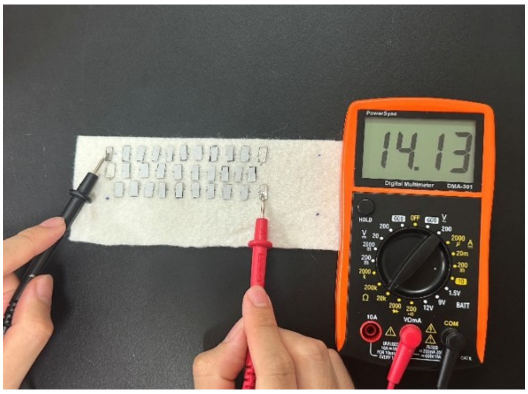

Fig. S9. Electrical resistance of the wearable TEGs comprising 30 pairs of p-n junctions.

References:

1. H. Li, Y. Liu, S. Liu, P. Li, C. Zhang and C. He, *Compos A Appl Sci Manuf*, 2023, **166**, 107386.
2. T. Wu, X.-L. Shi, W.-D. Liu, M. Li, F. Yue, P. Huang, Q. Liu and Z.-G. Chen, *Adv. Fiber Mater.*, 2024, **6**, 607-618.
3. N. Wen, Z. Fan, S. Yang, Y. Zhao, C. Li, T. Cong, H. Huang, J. Zhang, X. Guan and L. Pan, *Chem. Eng. J.*, 2021, **426**, 130816.
4. C. Xu, S. Yang, P. Li, H. Wang, H. Li and Z. Liu, *Compos. Commun.*, 2022, **32**, 101179.
5. X. Yang and K. Zhang, *ACS Appl. Mater. Interfaces*, 2022, **14**, 44704-44712.
6. C. Zhang, Q. Zhang, D. Zhang, M. Wang, Y. Bo, X. Fan, F. Li, J. Liang, Y. Huang, R. Ma and Y. Chen, *Nano Lett.*, 2021, **21**, 1047-1055.
7. S.-J. Kim, Y. Kim and W.-R. Yu, *Nano Energy*, 2025, **140**, 111054.
8. M. T. Z. Myint, T. Nishikawa, K. Omoto, H. Inoue, Y. Yamashita, A. K. K. Kyaw and Y. Hayashi, *Sci. Rep.*, 2020, **10**, 7307.